Marine Geology 357 (2014) 392–400

Contents lists available at ScienceDirect

Marine Geology

journal homepage: www.elsevier.com/locate/margeo

Cretaceous–Paleogene boundary exposed: Campeche Escarpment, Gulf of Mexico

Charles K. Paull [a,*], David W. Caress [a], Roberto Gwiazda [a], Jaime Urrutia-Fucugauchi [b], Mario Rebolledo-Vieyra [c], Eve Lundsten [a], Krystle Anderson [a], Esther J. Sumner [a]

[a] Monterey Bay Aquarium Research Institute, Moss Landing, CA, USA
[b] Universidad Nacional Autónoma de México, México D.F.
[c] Centro de Investigación Científica de Yucatán, México

ARTICLE INFO

Article history:
Received 19 June 2014
Received in revised form 24 September 2014
Accepted 12 October 2014
Available online 30 October 2014

Keywords:
Cretaceous/Paleogene boundary
Debris flows
Chicxulub impact
Carbonate escarpments

ABSTRACT

We present the first multibeam bathymetric maps of the Campeche Escarpment, a Mesozoic carbonate platform in the Gulf of Mexico, which represents the closest Cretaceous–Paleogene (K-Pg) boundary outcrops to the Chicxulub impact structure. The impact of an extraterrestrial-body ~65 million years ago on top of this platform is implicated in the end of the Cretaceous mass extinction and caused the largest debris flow yet described on Earth, which is found across the floor of the Gulf of Mexico and the Caribbean Sea. The location of the K-Pg boundary has been identified in the escarpment face by combining the new multibeam data with existing information from boreholes. The boundary is represented by an abrupt change in gradient on the escarpment face. The morphology of the escarpment combined with seismic data reveals that a significant amount of material is missing from the face, which failed catastrophically due to seismic shaking produced by the impact. The escarpment face is inferred to be an important source for the extensive debris flows triggered by the impact, whose deposits are found throughout much of the Gulf of Mexico.

1. Introduction

The Campeche Escarpment of the Yucatan Peninsula, Mexico (Fig. 1), forms the steep northern edge of the continental margin that separates the shallow carbonate platform and ramp, which has persisted since the Mesozoic, from the deep waters of the Gulf of Mexico (e.g., Bryant et al., 1969). The Campeche Escarpment is ≥230 km from the center of the >180 km diameter Chicxulub impact structure (Fig. 1), one of the largest known impact structures on Earth (Morgan and Warner, 1999; Denne et al., 2013). The Chicxulub impact structure was produced when an extraterrestrial body struck the submerged platform (e.g., Hildebrand et al., 1991; Schulte et al., 2010). The complex structure comprises multiple rings inferred from a concentric circular pattern of gravity and magnetic anomalies, with approximate center near the present day coastline of the Yucatan Peninsula (Hildebrand et al., 1991; Sharpton et al., 1993; Morgan et al., 1997; Christeson et al., 2009). The impact is thought to have had profound consequences for the entire Earth, including a global environmental crisis that resulted in the mass extinction that marks the end of the Cretaceous Period (Alvarez et al., 1980; Smit and Hertogen, 1980; Schulte et al., 2010).

The Chicxulub impact structure, now buried by up to 1 km of Cenozoic sediments, has been identified by gravity, magnetic, seismic reflection, and seismic refraction studies (e.g., Sharpton et al., 1993; Morgan et al., 1997; Christeson et al., 2009; Gulick et al., 2013). A few boreholes located within the impact structure have penetrated the Cenozoic cover and sampled the impact breccias and deposits that refilled the crater (Urrutia-Fucugauchi et al., 1996, 2004, 2008, 2011; Rebolledo-Vieyra et al., 2000; Rebolledo-Vieyra and Urrutia-Fucugauchi, 2004). These observations combined with modeling (Collins et al., 2002, 2008) have enabled the reconstruction of the impact event.

The impact vaporized and ejected kilometers of crust, produced a transient cavity extending down to the Moho discontinuity, and deformed the upper mantle (Christeson et al., 2009). Within minutes, this cavity was refilled by plumes of material rising from the underlying mantle and by collapse of the surrounding carbonate platform (e.g., Morgan and Warner, 1999; Gulick et al., 2008, 2013; Christeson et al., 2009). The crater also filled with a melt sheet, ejecta, sidewall slope failure blocks, and tsunami deposits (Gulick et al., 2013; Whalen et al., 2013). A ring of faults extending at least 130 km away from the crater's center have up to 300 m of vertical displacement. These faults were caused by the collapse of the platform and partially refilled the 30 km deep transient cavity (Morgan et al., 1997; Morgan and Warner, 1999).

The impact generated shock waves with the energy equivalent to a magnitude 12+ earthquake on the Richter scale (Collins et al., 2002), initiated huge tsunamis, and triggered slope failures. This caused profound devastation throughout the North American southeast and

* Corresponding author.
E-mail address: Paull@mbari.org (C.K. Paull).

http://dx.doi.org/10.1016/j.margeo.2014.10.002

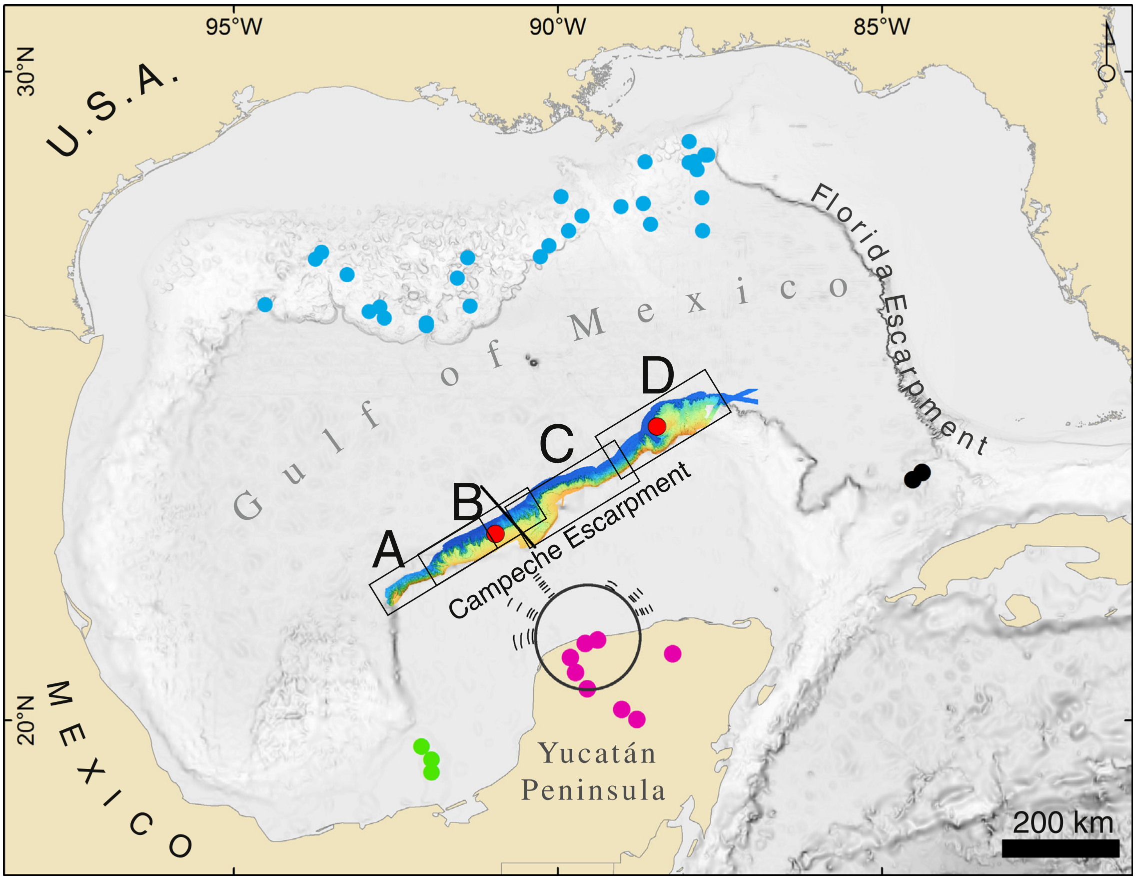

Fig. 1. Map showing location of multibeam survey covering the Campeche Escarpment (indicated with color shaded depths) with respect to the Chicxulub impact crater (black circle), Yucatan Peninsula, Florida Escarpment, and Gulf of Mexico. Black dashes surrounding the crater indicate locations of ring faults (after Gulick et al., 2013). Black rectangles outline sections of map shown in more detail in Fig. 2A–D. The location of DSDP Sites 86 and 94 are shown with filled red circles. Location of sites with the most proximal K-Pg deposits are also indicated with filled circles (boreholes south of impact structure after Rebolledo-Vieyra et al., 2000, purple; Cantarell Oil Field after Grajales-Nishimura et al., 2000, green filled circles; DSDP Sites 534 and 535 after Bralower et al., 1998, black filled circles; and industry boreholes in the northern Gulf of Mexico after Denne et al., 2013, blue filled circles). Location of seismic profile GT-3-60, on which Fig. 5 is based, is shown with thin black line.

Caribbean (e.g., Smit et al., 1996; Bralower et al., 1998; Norris and Huber, 1999; Goto et al., 2008; Schulte et al., 2012; Denne et al., 2013) and left behind K-Pg boundary deposits that are meters to more than one hundred meters thick (Bourgeois et al., 1988; Alvarez et al., 1992; Smit et al., 1996; Bralower et al., 1998; Norris and Huber, 1999; Claeys et al., 2002; Arenillas et al., 2006; Goto et al., 2008; Urrutia-Fucugauchi et al., 2008; Denne et al., 2013). The deposits comprise variable mixtures of ejecta, breccia, tsunami deposits, debris flow deposits (debrites), and airfall material.

The morphology and stratigraphy of the Yucatan Peninsula to the north of the Chicxulub impact structure and in particular on the Campeche Escarpment are not well known. However, similar steep carbonate escarpments (e.g., Florida and Blake-Bahama Escarpments) are erosional features where the truncated edges of the nearly flat-lying Cretaceous strata of the adjacent carbonate platforms are exposed (e.g., Dillon et al., 1987, Paull et al., 1990a, b).

Few multichannel seismic reflection profiles are available that cross the Campeche Escarpment and reveal its internal structure. Locker and Buffler (1983) published two profiles in an article contrasting the Campeche and Florida escarpments: two ostensibly analogous carbonate platforms on the southern and eastern sides of the Gulf of Mexico, respectively. They note that the edge of the Campeche Escarpment is significantly more complex than the Florida Escarpment. A prominent strong reflector surface outside the impact structure, with considerable topography, extends at least 50 km from the lower Campeche Escarpment face. This reflector is identified as the Mid-Cretaceous Unconformity (MCU), a hiatus separating lower Cretaceous from early Cenozoic strata (Locker and Buffler, 1983). Faults occur beneath the MCU with >100 m of throw; which was surprising prior to the discovery of the Chicxulub impact structure (Locker and Buffler, 1983) because this is a stable region tectonically (Alvarez et al., 1980; Smit and Hertogen, 1980; Hildebrand et al., 1991).

In 1970, Deep Sea Drilling Project (DSDP) Leg 10 located two boreholes (Sites 86 and 96) on the Campeche Escarpment. They retrieved apparently complete Paleogene sections rich in pelagic carbonates that ended in a hard formation, which yielded ~1% recovery and was composed of oddly orange stained shallow water carbonate facies containing Early Cretaceous fossils (Worzel et al., 1973). At the time, the existence of the Chicxulub impact structure was not general knowledge, and its potential association with the K-Pg boundary was yet to be realized (Alvarez et al., 1980; Hildebrand et al., 1991). As a result no consideration was given to whether the recovered Early Cretaceous fossils were in situ or impact ejecta (Worzel et al., 1973).

Fig. 2. Panels A–D show the bathymetry of the Campeche Escarpment as indicated in Fig. 1. Red boxes indicate areas shown in more detail in Figs. 3 and 4. A perspective view from the direction indicated by the red arrow in panel A is shown in Fig. 4C. The location of seismic profile GT-3-60, in which Fig. 5 is based, is indicated with a black line in panels B and C. Sections of the escarpment characterized by gullies (G) are indicated with brackets.

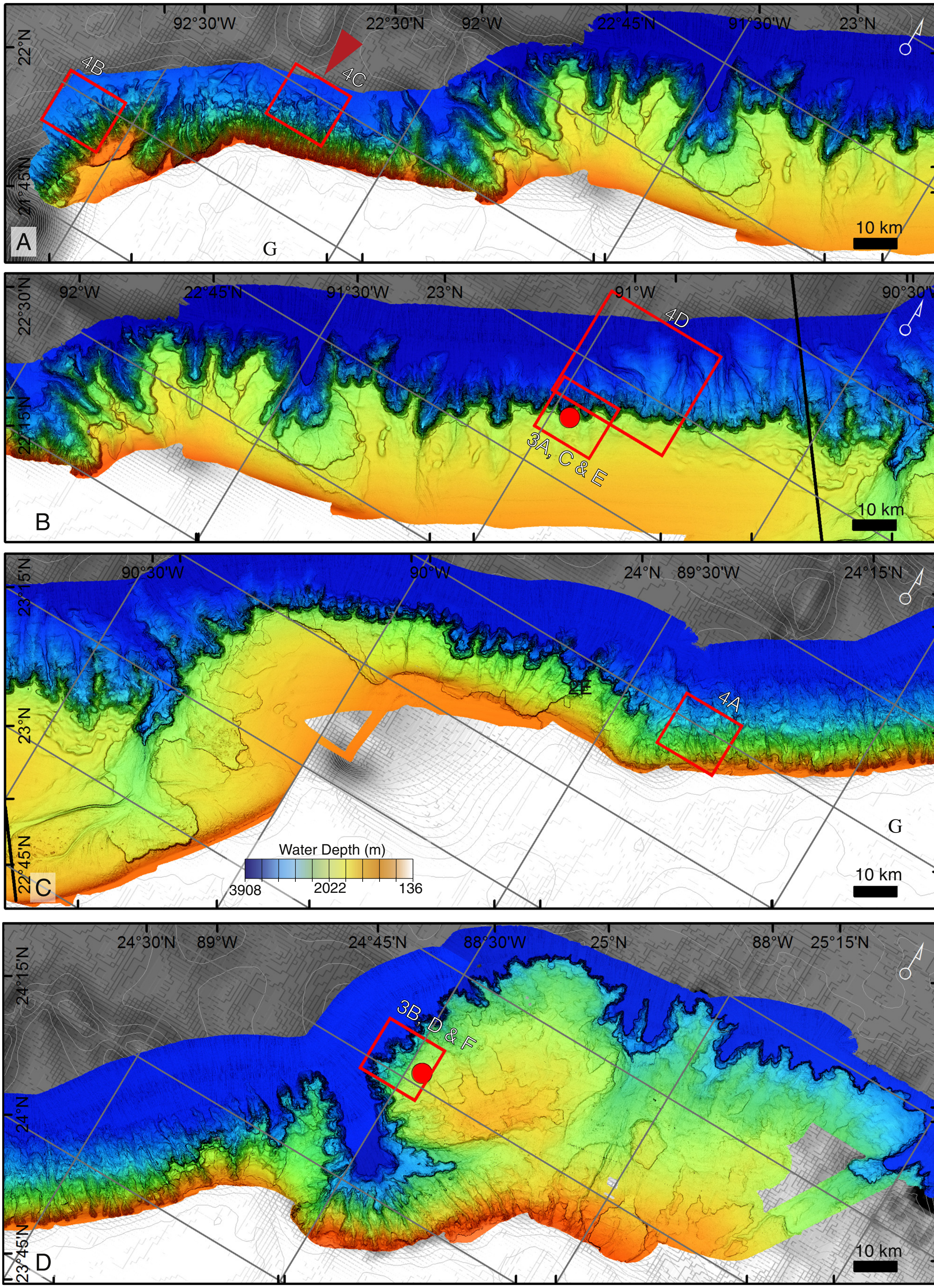

A
92°30'W
22°30'N
92°W
22°45'N
91°30'W
23°N
22°N
21°45'N
4B
4C
G
10 km
B
92°W
22°45'N
91°30'W
23°N
91°W
90°30'W
22°30'N
22°15'N
4D
3A, C & E
10 km
C
90°30'W
90°W
24°N
89°30'W
24°15'N
23°15'N
23°N
22°45'N
4A
G
Water Depth (m)
3908
2022
136
10 km
D
24°30'N
89°W
24°45'N
88°30'W
25°N
88°W
25°15'N
24°15'N
24°N
23°45'N
3B, D & F
10 km

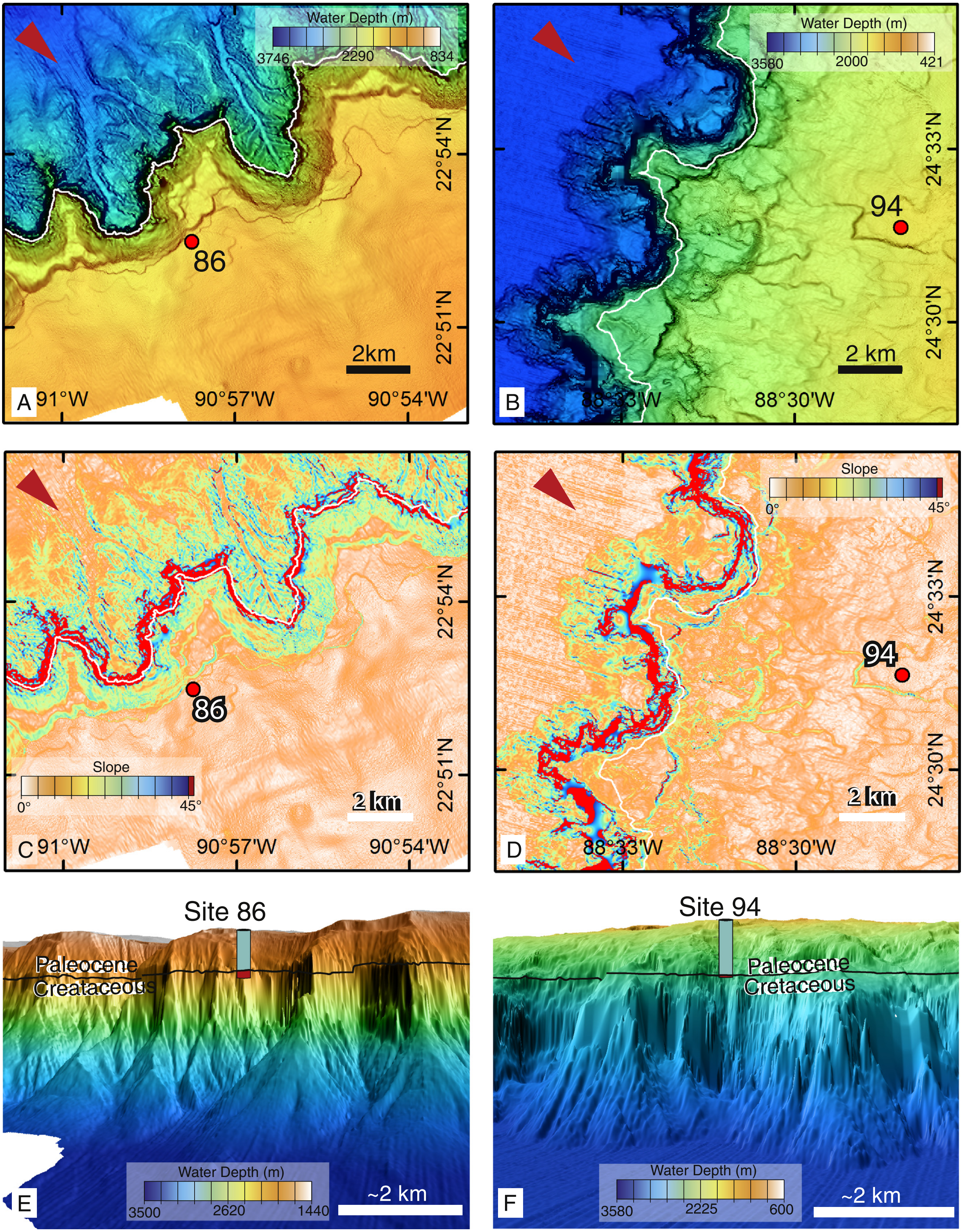
Water Depth (m)
3746
2290
834
22°54'N
22°51'N
86
2km
A
91°W
90°57'W
90°54'W
Water Depth (m)
3580
2000
421
24°33'N
24°30'N
94
2 km
B
88°33'W
88°30'W
C
Slope
0°
45°
2 km
D
Site 86
Paleocene
Creataceous
Water Depth (m)
3500
2620
1440
~2 km
E
Site 94
Paleocene
Cretaceous
3580
2225
600
F

The closest sampled offshore deposits attributed to the impact event are more than 600 km to the north and north east of the Chicxulub impact structure on the floor of the Gulf of Mexico (Fig. 1; Alvarez et al., 1992; Bralower et al., 1998; Denne et al., 2013). These deposits are from boreholes drilled during DSDP Leg 77 in 1981, prior to the realization of the existence of the Chicxulub impact structure and its connection with the K-Pg boundary (Alvarez et al., 1980; Hildebrand et al., 1991). Reinterpretation of the DSDP Leg 77 sites, alongside data from industry wells in the northern Gulf of Mexico, indicate that debrites associated with the K-Pg boundary are up to 200 m thick and occur basin wide (Alvarez et al., 1992; Bralower et al., 1998; Denne et al., 2013). These deposits are referred to as the Cretaceous–Tertiary Cocktail (Bralower et al., 1998), hereafter the K-Pg Cocktail, because they contain a distinctive mixture of ejecta, shallow water carbonate breccia bearing Cretaceous fossils, shallow water foraminifera sands, and matrixes of nannofossils from multiple faunal zones.

Denne et al. (2013) presented evidence that K-Pg Cocktail debrites on the floor of the Gulf of Mexico involve between ~59 and 259×10^6 km^3 of material making it the largest known debris flow deposit on Earth (Denne et al., 2013). They also estimate that between 43 and 116×10^6 km^3 of the material in the K-Pg Cocktail was derived from shallow water carbonate platforms and slope environments.

The most proximal samples identified as K-Pg deposits come from boreholes drilled onshore, where breccia dominated deposits that exceed 350 m in thickness occur up to 165 km to the south and southeast of the Chicxulub impact structure (Fig. 1; Urrutia-Fucugauchi et al., 1996; Rebolledo-Vieyra et al., 2000). A carbonate breccia up to 300 m thick forms the reservoir for the Cantarell Oil Field ~300 km to the WSW of the Chicxulub impact structure (Fig. 1). This breccia is interpreted to be the deposit of a K-Pg boundary debris flow that carried material ~30 km up the slope from the western side of the Yucatan Platform (Grajales-Nishimura et al., 2000).

The Campeche Escarpment is a likely source for at least some of the shallow-water carbonate found in the K-Pg Cocktail, as it is relatively close (i.e., ≥230 km) to the Chicxulub impact structure (Christeson et al., 2009) and comprises shallow water carbonate (Bryant et al., 1969; Worzel et al., 1973). However, the Campeche Escarpment has received little academic attention as a potential source of debris flows. No detailed bathymetry was previously available, which is critical to evaluating whether it is a plausible source area, whether strata associated with the impact are currently exposed at the seafloor, and whether strata associated with the K-Pg boundary contain impact related alteration.

The first science expedition of the Schmidt Ocean Institute on the *R/V Falkor* was dedicated to producing a detailed map of the Campeche Escarpment. The primary goal was to determine whether deposits associated with the K-Pg boundary are exposed on the seafloor along the Campeche Escarpment and if so what do they reveal about the impact event.

2. Methods

The *R/V Falkor* is equipped with Kongsberg EM302 30 kHz and EM710 70 kHz multibeam sonars mounted on a gondola that extends beneath the keel. Surveys were conducted along the 612 km long northern face of the Campeche Escarpment targeting the water-depth range between ~400 m and the escarpment base at ≤3,700 m. The first multibeam line was laid out to follow the base of the escarpment using existing satellite bathymetry (Smith and Sandwell, 1997). Subsequent tracks were steered to get overlapping swath data with the nominal 120° beam footprint of the EM302 system. This was accomplished by running between 4 and 16 swaths parallel to the general NE-SW trend of the Escarpment face. Sound velocity profiles (SVP) were determined with full water column casts of a Valport Midas time of flight sensor at both ends of this initial survey line. Expendable bathythermograph (XBT) measurements on the upper 750 m of the water column were made twice a day and more frequently when the SVP sensor on the sonar gondola and the sound velocity profile being used in the Kongsberg systems differed by more than 5 m/sec. The data were processed using MB-System (Caress and Chayes, 1996). The EM710 system provides useful data in water depths shallower than 1,200 m, but no attempt was made to obtain full coverage with this sonar. The full 25-m grid resolution of these data is available via Google Earth and the raw data are available through Integrated Earth Data Applications (http://www.marine-geo.org/tools/search/entry.php?id=FK007).

3. Results

Multibeam data were collected along 5,898 km of track lines within the survey area, which provided 26,685 km^2 of state-of-the-art bathymetric coverage. The multibeam bathymetric survey reveals the morphology of the entire 612 km northern face of the Campeche Escarpment from ~400 m water depths to the floor of the abyssal Gulf of Mexico in ~3,700 m water depths (Fig. 2). Two distinctive textures occur along the face of the Campeche Escarpment that are distinguished by the size of the down slope cutting features (here the larger features are called canyons and the smaller, narrower features are called gullies) and the continuity of the slope gradients on the escarpment.

The most common morphology along the face of the Campeche Escarpment is characterized by a series of canyons cutting into the escarpment face. These segments of the Campeche Escarpment commonly have 5° slopes above ~2–2.5 km depth with an abrupt change to >25° slopes below (Figs. 1–3). The steep lower escarpment is indented by ~80 submarine box canyons. These box canyons occur within ~500 m high cliffs that form semicircular U-shaped amphitheater-like headwalls below ~2–2.5 km water depths (Figs. 2 and 3). The existence of most of these canyons was not known prior to this survey. The steep cliff face can be traced laterally along two segments of the escarpment face that are 290 and 190 km long (Fig. 2). The steepness and lateral continuity of the cliff faces suggests that the face of the escarpment is largely free from sediment drape.

Although multiple channels occur within the canyon fill below the ~500 m high cliffs, only one canyon has a well-developed channel that cuts across the face of the cliff and extends onto the gentler slopes above. The gentle slopes are marked with scarps that outline large slope failures.

The other distinctive texture on the face of the Campeche Escarpment occurs in two segments of the escarpment that are 90 and 105 km in length. It is characterized by having a continuous ~9° slope that persists from ≤500 mbsl to the base of the escarpment (Figs. 2 and 4A, B). These slopes are cut by numerous v-shaped gullies, which results in a corrugated appearance. The gullies extend from the upper slope down to the basin floor without a consistent regional break in slope, which suggests a lack of outcropping layers. The boundary between the two textures (canyon versus gulley) occurs where the gullied segments are recessed with respect to the adjacent canyon-bearing segments.

Fig. 3. Parts A–F show the most common escarpment morphology characterized by a steep cliff on the lower escarpment that is incised with submarine canyons with semicircular headwalls (locations indicated in Fig. 2). The projected location of the K-Pg boundary on the face of Campeche Escarpment (represented by the 2,050 mbsl white contour in parts A and C, and a black contour in E; and the 2,430 mbsl white contour in parts B and D, and a black contour in F) shows boundary corresponds with at distinct break in slope. Parts A and B are color scale bathymetric maps. Parts C and D are slope maps of the same areas as A and B, respectively, with 0 to 45° slopes in the white to blue scale and >45° slopes in red. DSDP Leg 10 Sites 86 and 94 (indicated with red filled circles in A–D) are located on the upper escarpment, but near the distinct change in slope associated with the lower escarpment. Parts E and F are perspective views from the direction indicated by the red arrows in parts A and B showing the projection of the K-Pg contact from DSDP Sites 86 and 94 respectively onto the escarpment face.

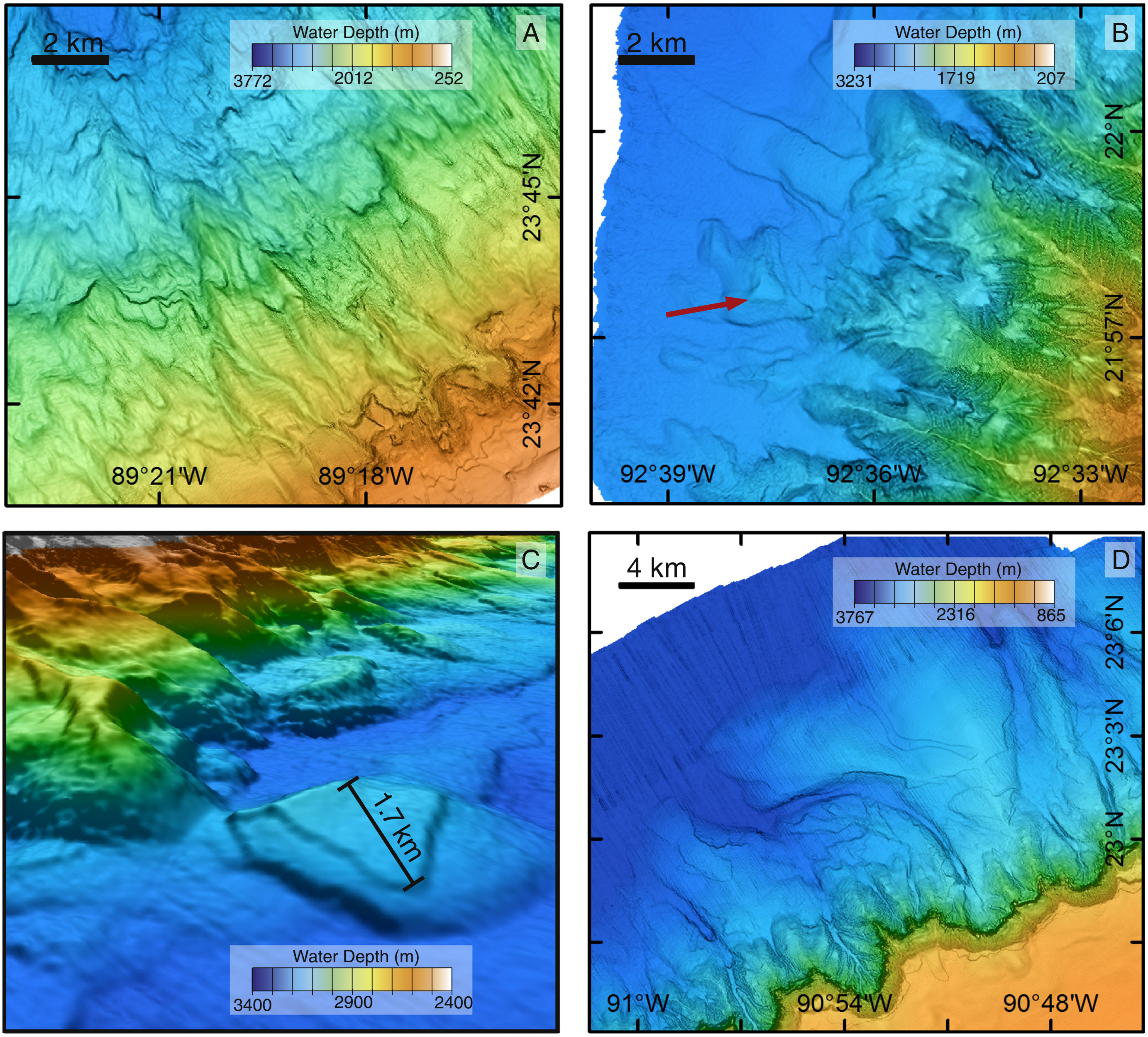

Fig. 4. Parts A–D show morphology of illustrative sections of the Campeche Escarpment (indicated in Fig. 2) in detail. Parts A and B are map views of the gullied morphology that characterizes approximately one third of the escarpment. Note the lack of the distinct break in slope separating a lower and upper escarpment. Red arrow in B shows topographic high on debris apron that is interpreted to be a large block. Part C is a perspective view showing a 1.7 km across block on the apron at the base of the escarpment. Part D shows a right angle bend in a channel developed on the apron at the base of the escarpment.

The base of the escarpment occurs where the nearly flat-lying abyssal sediments associated with the toe of the distal Mississippi Fan bury the foot of the Campeche Escarpment. In places, an apron of material exists between the flat-lying abyssal sediments and the steep lower face of the escarpment, which laps up onto the lower escarpment. This apron has a distinct blocky texture and appears to be composed of huge mega breccia blocks that are up to 2 km across and in places protrude through the abyssal fill (Fig. 4B, C). Right angle bends occur in the channels that cross the apron on the lower escarpment (Fig. 4D).

4. Discussion

4.1. Campeche Escarpment: stratigraphy and structure

The morphology of the steep slopes on the lower Campeche Escarpment indicates that the truncated edge of a massive rock unit outcrops along the face of this cliff. A distinct break in slope on the escarpment face at the top of this massive unit forms a horizon that can be traced along most of the escarpment (Figs. 2 and 3).

Control on where the K-Pg boundary crops out along the face of the Campeche Escarpment is provided by DSDP Leg 10 drilling results (Worzel et al., 1973). DSDP Site 86 was drilled in 1,462 m water depths within 200 m of the edge of a terrace overlying the steep face of the lower escarpment (Fig. 3A, C, E). Site 86 penetrated 672 mbsf (meters below seafloor) and collected 14 spot cores. The upper 9 cores contained nannofossil ooze, suggesting that the Cenozoic section was deposited in open marine conditions and lacked indications of significant hiatuses. An abrupt transition occurred between the Early Paleocene nannofossil ooze found in Site 86 Core 9 (2,013–2,022 meters below sea level [mbsl] with 3 m recovery), and the fragments of dolomite believed to be recrystallized shallow water calcarenites of Early Cretaceous age encountered in Site 86 Core 10 (2,072–2,081 mbsl with 0.3 m recovery). The gap between these cores pins the depth of the base of the Paleocene to between 2,016 and 2,081 mbsl.

Similarly, DSDP Site 94 was drilled on a terrace ~5.5 km from the steep face of the lower escarpment in 1,793 m water depths (Fig. 3B, D, F). The first 36 of the 40 spot cores that were taken contained nannofossil ooze, again showing that the Cenozoic section was deposited in an open marine setting and is potentially complete. An abrupt change occurred between the Early Paleocene nannofossil ooze encountered in Core 36 (2,420–2,427 mbsl; with 7 m recovery) and Core 38 (2,428–2,436 mbsl; with 1 m recovery), where dolomites inferred to have been deposited in the interior of a shallow water carbonate platform of Early Cretaceous age were encountered. Core 37 had no recovery. The gap between Cores 36 and 38 pins the depth of the base of the Paleogene nannofossil ooze to be between 2427 and 2436 mbsl.

Because DSDP Sites 86 and 94 were both drilled near the edge of the platform, the position of the K-Pg boundary can be projected laterally to the escarpment face. In both areas, the projected top of the Cretaceous sequences corresponds with the break in the slope of the cliff face and the top of an ~500 m high cliff. While the stratigraphy of DSDP Sites 86 and 94 helps constrain the location of the boundary between the Paleogene sediments and the underlying deposits containing at least fragments of Cretaceous age material, whether the recovered Cretaceous material is composed of meteorite impact ejecta or in-place Cretaceous strata remains unclear. The observed lithologic change in DSDP Sites 86 and 94 is consistent with the pre-Paleogene deposits being the cliff-forming unit. The break in slope provides a traceable horizon that can be identified along two thirds of the escarpment face (Figs. 2 and 3C, D). With increasing distance from the boreholes, the K-Pg boundary crosses isobaths (Fig. 3C, D), suggesting that there is either a modest regional dip or some topography on the surface of this unconformity.

The occurrence of faults with substantial throws (~100 m), revealed in the isolated multichannel seismic reflection profiles across the Campeche Escarpment, was noted as being perplexing by Locker and Buffler (1983; line NECE-9) as this is an otherwise tectonically quiet region. These structures primarily terminate at the MCU. In retrospect, the possibility that the observed shelf edge structure is attributable to the impact event should be considered. The faults indicated by Locker and Buffler (1983) now seem modest with respect to the >300 m displacement along the ring faults since imaged on the platform closer to the impact structure (Morgan et al., 1997; Morgan and Warner, 1999; Gulick et al., 2008, 2013).

Locker and Buffler (1983) show that the reflector identified outside the impact structure as the MCU rises ~800 m (0.9 seconds twt) ~50 km from the edge of the lower escarpment, near the present shelf edge (Fig. 5). This was originally interpreted as being a ~50 km depositional

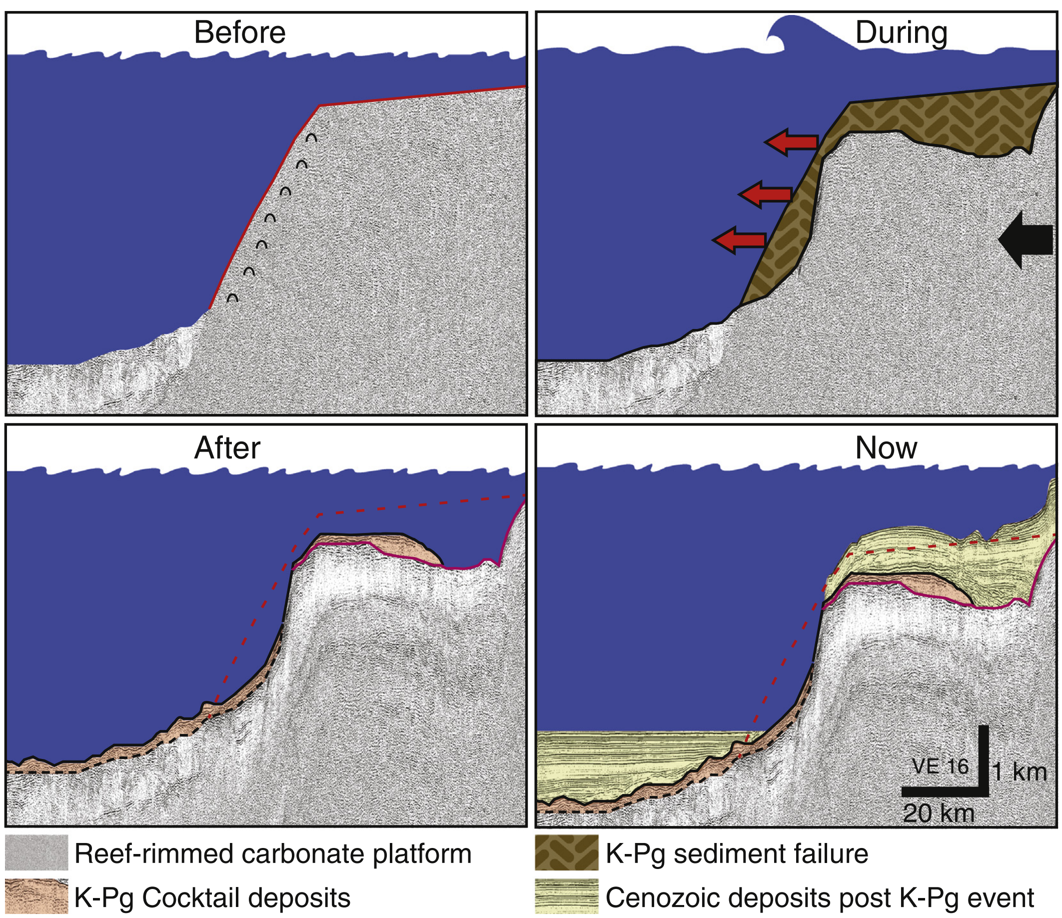

Fig. 5. The effect of the K-Pg event on the Campeche Escarpment and its subsequent Cenozoic evolution is illustrated with a cartoon. The pre-impact continental margin is inferred to be a reef-rimmed carbonate platform (Before). Seismic waves from the impact resulted in the collapse of the face of the escarpment (During). The sections of the escarpment face and continental shelf adjacent to the escarpment that failed during the event are illustrated with brown shading. The failed material was transported into the basin by gravity flows, becoming a major contributor to the thick K-Pg Cocktail deposits (orange shading) over the floor of the Gulf of Mexico (After). A schematic interpretation based on multichannel seismic reflection profile GT-3-60 after Locker and Buffler (1983) shows modern conditions (Now). Cenozoic sediments (yellow shading) now cover the K-Pg deposit on the floor of the Gulf of Mexico and the surface of the Yucatan Platform. The MCU on the platform is indicated with the pink line. K-Pg Cocktail deposits are inferred to occur on the surface of the MCU and may be exposed along much of the Campeche Escarpment (Panels C and D). This seismic line (GT-3-60; made available through the UTIG Seismic Data Center (Shipley et al., 2012) also crosses the only canyon that is incised into the upper escarpment, which further complicates the stratigraphy (Fig. 2B, c). The vertical exaggeration is 16. The new bathymetry shows the profile crossed the lower escarpment on the flank of a canyon, which produced distracting side echo artifacts that have been whited-out for this illustration.

step back in the position of the carbonate platform edge, presumably associated with unknown paleooceanographic changes in the Cretaceous, which corresponded with the MCU. Retreats in the positions of carbonate platform edges are puzzling as shallow water carbonate platforms characteristically experience prolific sediment production which easily keeps pace with long-term subsidence especially in tectonically quiet regions (Schlager, 1981; Mullins et al., 1991). Conversely, the observed shelf edge retreat may be the scar of a massive slope failure. A scar of this size (50 km wide involving up to 0.8 thick section, which extends for 100 km along the escarpment face) would only involve ~4,000 km^3 of material, which represents a modest contribution to the total volume of material inferred to be within the K-Pg Cocktail on the floor of the Gulf of Mexico (Denne et al., 2013). Moreover, the observation of an abrupt change from the shallow water carbonate facies below the MCU to the sudden onset of an apparently continuous Paleogene pelagic sequence above is consistent with the MCU being generated by a massive slide scar during the K-Pg event (Fig. 5).

4.2. Campeche Escarpment: source for massive K-Pg debris flow

The volume of material that may have failed from the edge of the entire Yucatan Platform during the K-Pg event and contributed to the K-Pg Cocktail on the floor of the Gulf of Mexico (Denne et al., 2013) needs to be considered. Impacts with large extraterrestrial bodies have been identified as the triggering mechanism for other gigantic submarine mass transport deposits (e.g., Deptuck and Campbell, 2012). The estimated 43 to 116×10^6 km^3 of material contained within the floor of the Gulf of Mexico is the largest known mass transport deposit on Earth (Denne et al., 2013).

The WSW (Grajales-Nishimura et al., 2000) and ENE (Alvarez et al., 1992; Bralower et al., 1998) flanks of the platform, which were not covered in the recent survey, are likely additional contributors to the massive debris flow. Thus, the likely total source region on the flanks of the Yucatan Platform was ~1,300 km long. If the Yucatan Platform is the sole source area, and the escarpment was 3 km high prior to the impact, 11 km of lateral retreat on the entire face of the Campeche Escarpment is required to provide 43×10^6 km^3 of material. Shallow water carbonates rimmed most of the perimeter of the Gulf of Mexico in the Cretaceous, providing an additional ~2,200 km-long potential source area. If shallow water carbonates from along the entire margin of the Gulf of Mexico contributed material to the K-Pg Cocktail, a volume of material equivalent to minimum 4 km of lateral retreat along the entire edge of the Yucatan Platform would still be required. These simple calculations suggest that the face of the Campeche Escarpment was massively altered during the impact event (Fig. 5) and might explain why platform edge facies are absent from the Florida Escarpment as well (Paull et al., 1990a).

The apron, which is exposed in places along the lowermost flank of the escarpment, is interpreted to be K-Pg Cocktail material that overlays the still intact platform edge. Mega breccia blocks that are ~2 km across are still identifiable within the apron (Fig. 4B, C). The right angle diversions in the orientations of channels that cross this apron may reflect channel deflection associated with individual breccia blocks. Seismic profiles suggest that this apron is hundreds of meters thick (Locker and Buffler, 1983). This apron is interpreted to be the most proximal pieces of the debris flow material that collapsed into the Gulf of Mexico Basin following the impact. The K-Pg Cocktail apron (Fig. 5) and mega breccia blocks attest to the scale of platform edge failures that occurred along the Campeche Escarpment face presumably during the impact event.

5. Conclusions

Multibeam bathymetry reveals the detailed shape of the Campeche Escarpment for the first time and provides new insight into how the Chicxulub impact event affected the edge of the Yucatan Platform. A steep cliff occurs on the lower escarpment and can be traced along the majority of the escarpment face. Correlations with boreholes drilled during DSDP Leg 10 indicate that the top of this cliff corresponds with the K-Pg boundary and the face of the cliff corresponds with the underlying deposits found to contain fragments of lower Cretaceous age. Whether the pre-Cenozoic material recovered in these DSDP boreholes is composed of impact ejecta or in-place Cretaceous strata, and if indeed an ejecta blanket does extend to the platform edge is unknown. The Campeche Escarpment face is the probable source for a major component of the material carried in the mega debris flow that filled the floor of the Gulf of Mexico. By inference, several km of lateral retreat of the escarpment face may have occurred during the K-Pg event.

Acknowledgments

The Schmidt Ocean Institute provided the R/V Falkor cruise. David and Lucile Packard Foundation also provided support. We thank Sean Gulick, David Piper, and an anonymous reviewer for their helpful suggestions.

References

Alvarez, L., Alvarez, W., Asaro, F., Michel, H.V., 1980. Extraterrestrial cause for the Cretaceous–Tertiary extinction. Science 208, 1095–1108.
Alvarez, W., Smit, J., Lowrie, W., Asaro, F., Margolis, S.V., Claeys, P., Kastner, M., Hildebrand, A.R., 1992. Proximal impact deposits at the Cretaceous–Tertiary boundary in the Gulf of Mexico: A restudy of DSDP Leg 77 Sites 536 and 540. Geology 20, 697–700.
Arenillas, I., Arz, J.A., Grajales-Nishimura, J.M., Muñetón, Murillo-, Alvarez, W., Camargo-Zanoguera, A., Molina, E., Rosales- Domínguez, C., 2006. Chicxulub impact event is Cretaceous/Paleogene boundary in age: New micropaleontological evidence. Earth and Planetary Science Letters 249, 241–257.
Bourgeois, J., Hansen, T.A., Wiberg, P.L., Kauffman, E.G., 1988. A tsunami deposit at the Cretaceous–Tertiary boundary in Texas. Science 241, 567–570.
Bralower, T.J., Paull, C.K., Leckie, M.R., 1998. Massive sediment gravity flows in the Gulf of Mexico and Caribbean during the Cretaceous/Tertiary boundary event. Geology 26, 331–334.
Bryant, W.R., Meyerhoff, A.A., Brown, N.K., Furrer, M., Pyle, T., Antoine, J.W., 1969. Escarpments reef trends, and diapiric structures, eastern Gulf of Mexico. Bulletin of the American Association of Petroleum Geologists 53, 2506–2542.
Caress, D.W., Chayes, D.N., 1996. Improved processing of Hydrosweep DS multibeam data on the *R/V Maurice Ewing*. Marine Geophysical Researches 18, 631–650.
Christeson, G.L., Collins, G.S., Morgan, J.V., Gulick, S.P.S., Barton, P.J., Warner, M.R., 2009. Mantle deformation beneath the Chicxulub impact crater. Earth and Planetary Science Letters 284, 249–257.
Claeys, P., Kiessling, W., Alvarez, W., 2002. Distribution of Chicxulub ejecta at the Cretaceous–Tertiary boundary. In: Koeberl, C., MacLeod, K.G. (Eds.), Catastrophic Events and Mass Extinctions: Impacts and Beyond. Special Paper, 356, Geological Society of America, Boulder, pp. 55–68.
Collins, G.S., Melosh, H.J., Morgan, J.V., Warner, M.R., 2002. Hydrocode simulations of Chicxulub crater collapse and peak-ring formation. Icarus 157, 24–33.
Collins, G.S., Morgan, J., Barton, P., Christeson, G.L., Gulick, S., Urrutia Fucugauchi, J., Warner, M., Wünnemann, K., 2008. Dynamic modeling suggests terrace zone asymmetry in the Chicxulub crater is caused by target heterogeneity. Earth and Planetary Science Letters 270, 221–230.
Denne, R.A., Scott, E.D., Eickhoff, D.P., Kaiser, J.S., Hill, R.J., Spaw, J.M., 2013. Massive Cretaceous–Paleogene boundary deposit, deep-water Gulf of Mexico: New evidence for widespread Chicxulub-induced slope failure. Geology 41, 983–986.
Deptuck, M.E., Campbell, D.C., 2012. Widespread erosion and mass failure from the ~51 Ma Montagnais marine bolide impact off southwestern Nova Scotia, Canada. Canadian Journal of Earth Sciences 49, 1567–1594.
Dillon, W.P., Valentine, P.C., Paull, C.K., 1987. The Blake Escarpment — A product of erosional processes in the deep ocean, inCooper, R., Ed., National Oceanic and Atmospheric Administration, Symposium Series for Undersea Research, Washington D. C. 2, 177–190.
Goto, K., Tada, R., Tajika, E., Iturralde-Vincent, M.A., Matsui, T., Yamamoto, S., Nakano, Y., Oji, T., Kiyokawa, S., García Delgado, D.E., Diaz Otero, C., Rojas Consuegra, R., 2008. Lateral lithological and compositional variations of the Cretaceous/Tertiary deep-sea tsunami deposits in northwestern Cuba. Cretaceous Research 29, 217–236.
Grajales-Nishimura, J.M., Cedillo-Pardo, E., Rosales-Domínguez, M.C., Moran-Centeno, D.J., Alvarez, W., Claeys, P., Ruiz-Morales, J., Garcia-Hemandez, J., Padilla-Avila, P., Sanchez-Rios, A., 2000. Chicxulub impact: The origin of reservoir and seal facies in the southeastern Mexico oil fields. Geology 28, 307–310.
Gulick, S.P.S., Barton, P., Christeson, G.L., Morgan, J.V., McDonald, M., Mendoza-Cervantes, K., Pearson, Z.F., Surendra, A., Urrutia-Fucugauchi, J., Vermeesch, P.M., Warner, M.R., 2008. Importance of pre-impact crustal structure for the asymmetry of the Chicxulub impact crater. Nature Geoscience 1, 131–135.
Gulick, S.P.S., Christeson, G.L., Barton, P.J., Grieve, R.A.F., Morgan, J.V., Urrutia-Fucugauchi, J., 2013. Geophysical characterization of the Chicxulub impact crater. Reviews of Geophysics 51, 31–52.

Hildebrand, A.R., Penfield, G.T., Kring, D.A., Pilkington, M., Camargo, Z.A., Jacobsen, S.B., Boynton, W.V., 1991. Chicxulub crater: A possible Cretaceous/Tertiary boundary impact crater on the Yucatan Peninsula, Mexico. Geology 19, 867–871.
Locker, S.D., Buffler, R.T., 1983. Comparison of lower Cretaceous carbonate shelf margins, northern Campeche Escarpment and northern Florida Escarpment, Gulf of Mexico. American Association of Petroleum Geologists. Studies in Geology 15, 2.2.3-123–2.2. 3-128.
Morgan, J., Warner, M., 1999. Chicxulub: The third dimension of a multi-ring impact basin. Geology 27, 407–410.
Morgan, J., Warner, M., Chicxulub Working Group, 1997. Size and morphology of the Chicxulub impact crater. Nature 390, 472–476.
Mullins, H.T., Dolan, J., Breen, N., Anderson, B., Gaylord, M., Petruccione, J.L., Weller, R.W., Melillo, A.J., Jurgens, A.D., 1991. Retreat of carbonate platforms: Response to tectonic processes. Geology 19, 1089–1092.
Norris, R.D., Huber, B.T., 1999. Self-Trail, Synchronicity of the K-T oceanic mass extinction and meteorite impact: Blake Nose, western North Atlantic. Geology 27, 419–422.
Paull, C.K., Freeman-Lynde, R., Neumann, A.C., Gardemal, M., D'Argenio, B., Bralower, T., Marsella, E., 1990a. Geology of the strata exposed on the Florida Escarpment. Marine Geology 91, 177–194.
Paull, C.K., Spiess, F.N., Curray, J.R., Twichell, D., 1990b. Origin of Florida Canyon and the role of spring sapping on the formation of submarine box canyons. Geological Society of America Bulletin 102, 502–515.
Rebolledo-Vieyra, M., Urrutia-Fucugauchi, J., 2004. Magnetostratigraphy of the impact breccias and post-impact carbonates from borehole Yaxcopoil-1, Chicxulub impact crater, Yucatan, Mexico. Meteoritics and Planetary Science 39, 821–830.
Rebolledo-Vieyra, M., Urrutia-Fucugauchi, J., Marin, L.E., Trejo-Garcia, A., Sharpton, V.L., Soler-Arechalde, A.M., 2000. UNAM Scientific Shallow—drilling program of the Chicxulub impact crater. International Geology Review 42, 928–940.
Schlager, W., 1981. The paradox of drowned reefs and carbonate platforms. Geological Society of America Bulletin 92, 197–211.
Schulte, P., et al., 2010. The Chicxulub asteroid impact and mass extinction at the Cretaceous–Paleogene boundary. Science 237, 1214–1218.
Schulte, P., Smit, J.A.N., Deutsch, A., Salge, T., Friese, A., Beichel, K., 2012. Tsunami backwash deposits with Chicxulub impact ejecta and dinosaur remains from the Cretaceous–Paleogene boundary in the La Popa Basin, Mexico. Sedimentology 59, 737–765.
Sharpton, V.L., Burke, K., Camargo-Zanoguera, A., Hall, S., Marin, L., Urrutia-Fucugauchi, J., 1993. Chicxulub multiring impact basin: Size and other characteristics derived from gravity analysis. Science 261, 1564–1567.
Shipley, T., Gahagan, L., Johnson, K., Davis, M. (Eds.), 2012. Seismic Data Center. University of Texas Institute for Geophysics (http://www.ig.utexas.edu/sdc/).
Smit, J., Hertogen, J., 1980. An extraterrestrial event at the Cretaceous–Tertiary boundary. Nature 285, 198–200.
Smit, J., Alvarez, W., Montanari, A., Claeys, P., Grajales-Nishimura, J.M., 1996. Coarse-grained, clastic sandstone complex at the K/T boundary around the Gulf of Mexico: Deposition by tsunami waves induced by the Chicxulub impact? In: Ryder, G., Fastovski, D., Gartner, S. (Eds.), Geological Society of America Special Paper, 307, Boulder, pp. 151–182.
Smith, W.H.F., Sandwell, D.T., 1997. Global seafloor topography from satellite altimetry and ship depth soundings. Science 277, 1956–1962.
Urrutia-Fucugauchi, J., Marin, L., Trejo-Garcia, A., 1996. UNAM scientific drilling program of Chicxulub impact structure—evidence for a 300 kilometer crater diameter. Geophysical Research Letters 23, 1565–1568.
Urrutia-Fucugauchi, J., Morgan, J., Stöffler, D., Claeys, P., 2004. The Chicxulub Scientific Drilling Project (CSDP). Meteoritics and Planetary Science 39, 787–790.
Urrutia-Fucugauchi, J., Chavez-Aguirre, J.M., Pérez-Cruz, L., De la Rosa, J.L., 2008. Impact ejecta and carbonate sequence in the eastern sector of the Chicxulub crater. Comptes Rendus Geosciences 340, 801–810.
Urrutia-Fucugauchi, J., Camargo-Zanoguera, A., Perez-Cruz, L., Perez-Cruz, G., 2011. The Chicxulub multi-ring impact crater, Yucatan carbonate platform, Gulf of Mexico. Geofisica International 50, 99–127.
Whalen, M.T., Gulick, S.P.S., Pearson, Z.F., Norris, R.D., Perez Cruz, L., Urrutia Fucugauchi, J., 2013. Annealing the Chicxulub impact: Paleogene Yucatan carbonate slope development in the Chicxulub impact basin, Mexico. Society of Economic Paleontologists and Mineralogists. Special Publication 105. http://dx.doi.org/10.2110/sepmsp.105.04 (23 pp.).
Worzel, J.L., Bryant, W., et al., 1973. Initial Reports of the Deep Sea Drilling Project vol. 10. U.S. Government Printing Office, Washington DC (747 pp.).